Supporting Information

Enantiomeric Interactions between Thermotropic Liquid Crystals and Organized Monolayers of Tyrosine-Containing Dipeptides

Yiqun Bai and Nicholas L. Abbott

Department of Chemical and Biological Engineering

University of Wisconsin-Madison, Madison, WI 53706 USA

This supporting information contains additional figures and descriptions that (1) provide experimental detail regarding the fabrication of LC samples, (2) provide PM-IRRAS spectra used to confirm the adsorption of all dipeptides used in this study, (3) provide data to confirm the orientation of the easy axis of nematic 5CB on L-C-L-Y and L-C-L-[p]Y-decorated surfaces and (4) present the maps of twist angles for 5CB on L-C-L-Y and L-C-L-F.

Additional Detail Regarding Experimental Methods.

Preparation of PDMS elastomeric stamps and stamping of $C_{16}SH$

PDMS elastomeric stamps were cast against a silicon wafer that was coated with gold to aid in the release of the PDMS. Raised features (having dimensions 2 mm width and 1mm height) were defined by manually excising columns from the cured PDMS stamps. The stamps were soaked in a 2 mM ethanolic solution of hexadecanethiol ($C_{16}SH$) for 1 min and gently dried under a stream of nitrogen gas. The stamps were placed into conformal contact with an obliquely deposited gold film for 30 s. By stamping the gold surface first with a stamp containing horizontal features and subsequently with a stamp containing vertical features, square regions of bare gold (where no contact was made with the stamp) were defined and surrounded by a hydrophobic $C_{16}SH$ monolayer.

Measurement of the Orientations of LCs in LC Cells with a Reference Surface

Briefly, the optical cell containing the LC was placed between crossed polarizers with the input polarizer facing the reference surface. The easy axis of the LC on the $C_{15}SH$ reference surface was aligned to the input polarizer.[1] An iterative process was used to minimize the transmission of 546.5 nm light through the regions functionalized with $C_{16}SH$ on the analytic surface. This was accomplished by rotating the sample between the stationary polarizers, followed by rotation of the analyzer. The transmission of light was minimized at each of the iterations. Images were obtained using a polarized light microscope (BX60, Olympus) equipped with a rotating stage and a digital camera (2.8 f-stop, 1/1000 shutter speed, 640 x 480 resolution). Consistent settings of the light intensity were used (aperture set at one-half maximum, and lamp intensity set at four-tenths maximum) for individual samples. The lamp intensity was set at four-tenths maximum to ensure that the images did not saturate during rotation of the analyzer. The analyzer was rotated at 10^o increments, with images obtained at each analyzer position. The fraction of light transmitted through the optical cell, T_{wg}, was fit to the function

$$T_{wg} = cos^2(\Psi - \gamma)$$

where Ψ is the twist angle of the LC, and γ is the position of the analyzer relative to the input polarizer ($\gamma = 0 – 170^o$). The fit was performed at each pixel of the family of polarized images of each optical cell using an algorithm implemented in MATLAB (version 7.3.0, 2006b) to yield a two-dimensional matrix with elements representing the values of the twist angle at each pixel.

Measurement of the Orientations of LCs in Symmetric LC Cells

The twist angles of the LC were also measured in symmetric LC cells, where the top and bottom surfaces were decorated with the same dipeptides (ie. L-C-L-Y). We first positioned the sample

to obtain extinction in a reference $C_{16}SH$ region (ie. both top and bottom surfaces were $C_{16}SH$). Next, we rotated the circular stage and analyzer to obtain extinction in the dipeptide region. The rotation of the stage corresponds to the the easy axis of the LC in the case of high anchoring energies. The angle of the analyzer measures the total twist in the LC sample. However, we note that the final twist angle obtained contains a $\pi/2$ ambiguity, where the twist angle is exactly the measured angle Ψ, or the twist angle is actually $90-\Psi$. This $\pi/2$ ambiguity results because we do not know *a priori* the orientation of the easy axis of the LC on the L-C-L-Y-decorated surface, and thus cannot align the easy axis parallel to the input polarizer. The procedures used to iteratively determine the alignment of the stage and analyzer to obtain maximum extinction of light were identical to those used in measurements of the twist angles of LC in the LC cells with the reference surfaces (see above).

PM-IRRAS spectra

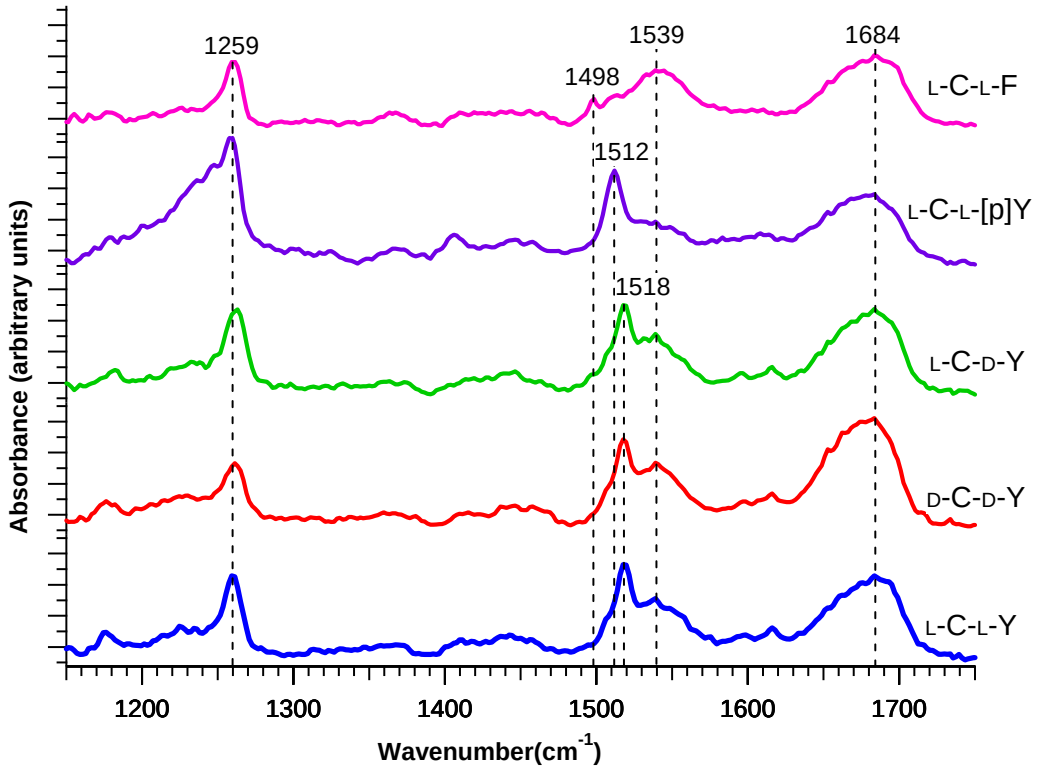

Figure S1. PM-IRRAS spectra of L-C-L-Y, D-C-D-Y, L-C-D-Y, L-C-L-[p]Y, and L-C-L-F. Each spectrum was acquired using 1000 scans on one sample.

Table S1. Peak assignments of dipeptides monolayers using PM-IRRAS.

Position	Molecule	Assignment	Reference
1259	All	Methyl rocking & C-C stretching	[2]
1498	L-C-L-F	C=C	[3,4]
1512	L-C-L-[p]Y	C=C	[5]
1518	L-C-L-Y, D-C-D-Y, L-C-D-Y	C=C	[3,6-8]
1539	L-C-L-Y, D-C-D-Y, L-C-D-Y, L-C-L-[p]Y	N-C=O (Amide II)	[9-11]
1684	L-C-L-Y, D-C-D-Y, L-C-D-Y, L-C-L-[p]Y	C=O (amide I)	[9-11]

Confirmation of the easy axis of nematic 5CB on dipeptide-decorated surfaces

Below we describe the results of experiments that sought to confirm our measurements of the easy axis of 5CB on surfaces reacted with L-C-L-Y and L-C-L-[p]Y. The conclusion that we measured the easy axis of 5CB dipeptide-decorated surfaces using LC samples formed by separating two surfaces by 50 μm is contingent on the assumption that the torque associated with the twist of the LC does not cause the director to depart from the easy axis of the LC on each surface. If, for example, the anchoring energy was significantly weaker on the surfaces prepared from L-C-L-Y as compared to L-C-L-[p]Y, one could also obtain the relative twist angles shown in Figure 5B on the basis of the effects of changes in anchoring energy. To address this possibility, we performed independent experiments to (1) confirm that the measured orientation of the director of the LC reported above is indeed the easy axis on each dipeptide decorated surface, and (2) confirm independently the orientations of the LC shown on each dipeptide surface, as reported in Figure 4B. To perform these experiments, we confined nematic 5CB between two surfaces that were identical (Figure S2A). We reasoned that if the orientation of the LC on the dipeptide-decorated surfaces obtained from the experiments described above are, in fact, the easy axes of the LC (i.e., we are not measuring the effects of differences in anchoring energies), we would be able to measure the same orientation of the LC in experimental systems where the twist of the LC differed from that reported in the experiments described above.

The LC cell shown in Figure S2A leads to regions of LC that are confined by surfaces with identical surface chemistries, namely either $C_{16}SH$, L-C-L-Y, or L-C-L-[p]Y, along the diagonal of the LC cell (Figure S2B). We make several observations that support our previous interpretation of the orientations of the easy axes of 5CB on the dipeptide-decorated surfaces. First, when using crossed polarizers with the sample oriented such that the $C_{16}SH$ and L-C-L-[p]Y

-decorated regions appeared dark, the L-C-L-Y -decorated region appeared bright (Figure S2B). This supports the previous results that the easy axis of L-C-L-Y is not parallel or perpendicular to the direction of gold deposition, and that the easy axis of L-C-L-[p]Y is close to the easy axis of $C_{16}SH$. Second, we sought to confirm that the easy axis of L-C-L-[p]Y was approximately perpendicular (82^o) from the direction of gold deposition. Because we know that the easy axis of $C_{16}SH$ is parallel to the direction of gold deposition, we compare the optical appearance of the LC in the CpY regions relative to the optical appearance of the LC in the $C_{16}SH$ regions. To determine whether the easy axes of $C_{16}SH$ and L-C-L-[p]Y were orthogonal to each other, we used a full wave plate (FWP) and observed the shift in the interference colors. We observed that upon inserting a FWP, the shift in the order of the interference colors were opposite for the $C_{16}SH$ and L-C-L-[p]Y -decorated regions (Figure S2C). This supports our conclusion that the easy axis of L-C-L-[p]Y is oriented 82^o from the direction of deposition of the gold film.

Through an additional experiment, we obtained further confirmation that the easy axis of L-C-L-Y was oriented 53^o away from the direction of gold deposition. For this experiment, we fabricated a symmetric cell using L-C-L-Y on the top and bottom surfaces. The schematic illustration of a symmetric cell created from L-C-L-Y is shown in Figure S3. If the easy axis of L-C-L-Y is not parallel or perpendicular to the direction of gold deposition, a LC cell created from these surfaces as shown in Figure S3 would result in a twisted LC cell, with the twist of the LC corresponding to twice the magnitude of the deviation of the orientation of the easy axis (measured from the $C_{16}SH$ direction). This was indeed observed (with the angles being $38.3^o \pm 1.7^o$, and $76.6^o \pm 3.2^o$, respectively) for 24 samples. We note that this method of determining the easy axis results in a $\pi/2$ ambiguity, thus the determined "easy axis" can be the η_0 or $90-\eta_0$. By combining the results from this experiment with the results from the previous method to obtain

the easy axis, we conclude that the easy axis is 90-38 = $52^{o}\pm 1.7^{o}$. This value is within the error of the previously measured easy axis of $53^{o}\pm 1.3^{o}$.

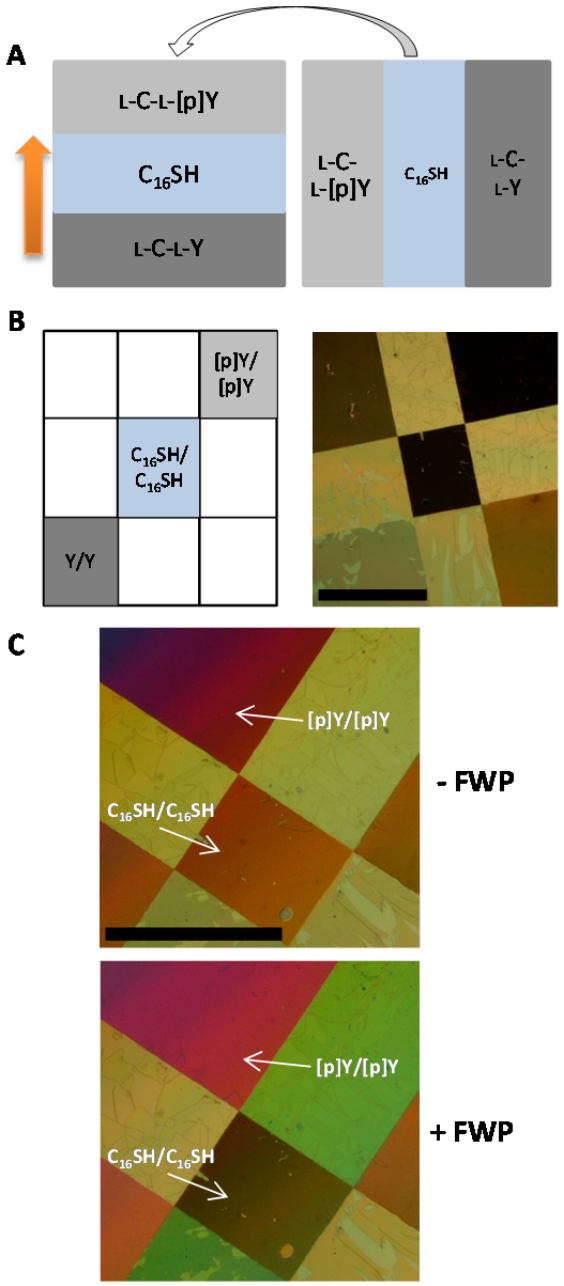

Figure S2. (A) Schematic illustration of the top and bottom surfaces used to create symmetric regions of L-C-L-Y/ L-C-L-Y, $C_{16}SH$/ $C_{16}SH$, and L-C-L-[p]Y/ L-C-L-[p]Y. (B) left: Schematic illustration of the assembled symmetric cell and right: optical image of the corresponding LC sample under cross polarizers. (C) Optical image of the LC sample depicted in (B) rotated 45° away from the position of maximum extinction (top), and with a FWP inserted into the light path (bottom). All scale bars are 2mm.

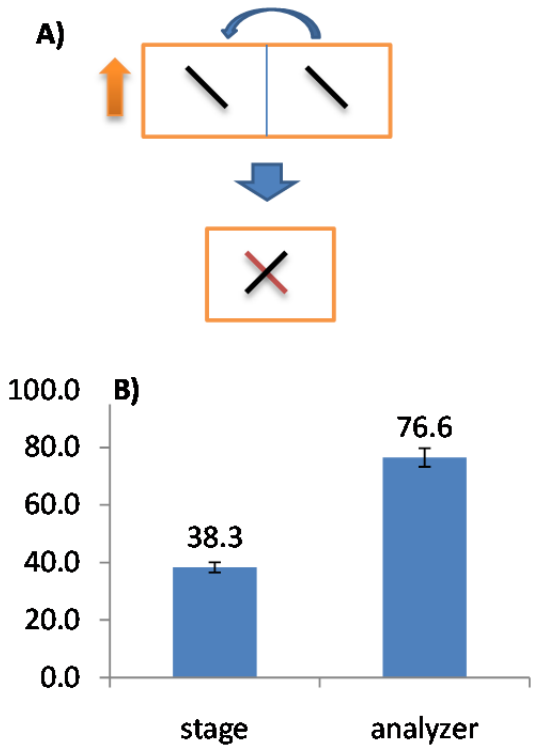

Figure S3. (A) Schematic illustration showing that a symmetric cell comprised of a surface with easy axis that is not parallel or perpendicular to the direction of gold deposition gives rise to a twist cell. (B) Quantitative analysis of the rotation of the stage and analyzer position needed to obtain extinction of a twist cell created from gold films incubated with L-C-L-Y.

Confirmation of the absence of peptide desorption into the LC

To confirm that the chiral dipeptides immobilized on the surface did not desorb into the LC (and thus act as a chiral dopant in the LC), we performed an experiment in which we created an optical cell from two surfaces supporting L-C-L-Y (symmetric cell, Figure S4). If the twist angles reported above were indeed a result of the easy axis, then the twist of the LC in the symmetric cell would depend on the relative orientations of the top and bottom surfaces. In particular, by arranging the top and bottom surfaces in an orthogonal orientation (Figure S4A), we expect to observe very little twist in the symmetric cell. As shown in Figure S3B, there was indeed little twist (2^{o}) in this symmetric cell, and further confirms that we measured twist angles that resulted from the easy axis of 5CB rather than a desorption of chiral dipeptides into the LC. We also performed an experiment in which we prepared a LC cell that varied in thickness (Figure S4C). If the twist angle induced in the LC was due to a chiral dopant in the bulk of the LC, the twist angle would be a function of the LC film thickness and thus vary across the cell. Only a variation in twist was observed at very thin locations in the sample (2 μm), where the torque applied to the liquid crystal is very high. In areas without substantial torque, this variation in twist of the LC was not observed in the experiments, thus providing confirmation that the twist in the LC described above is not due to desorption of the chiral dipeptides into the LC.

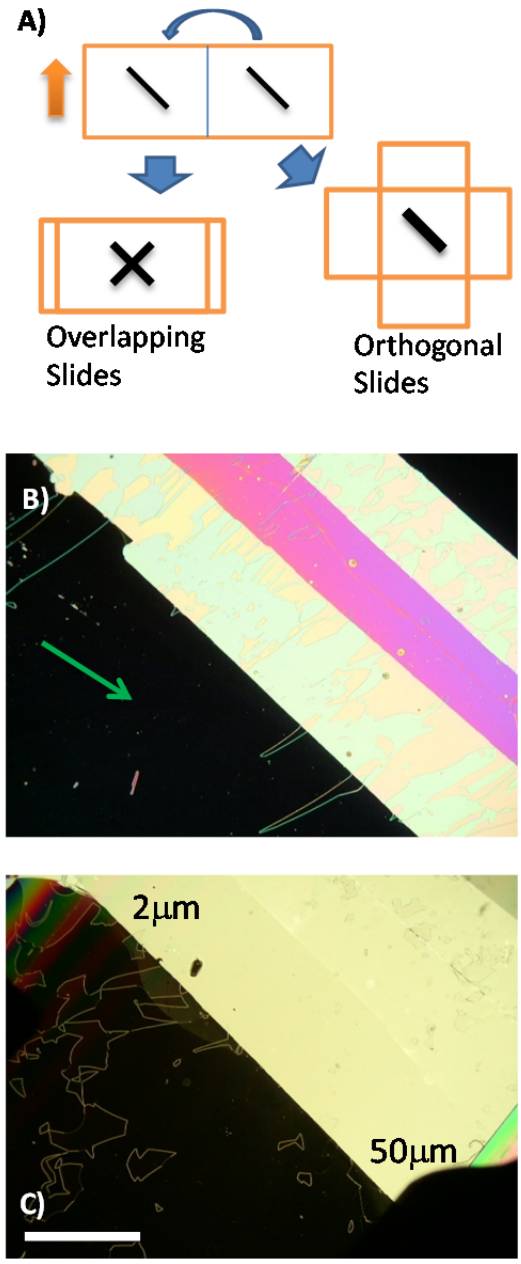

Figure S4. (A) Schematic illustration showing that a symmetric cell comprised of a surface with easy axis that is not parallel or perpendicular to the direction of gold deposition gives rise to a twist cell when the slides are directly overlapped. By assembling the surfaces orthogonally, the twist of the LC cell should be reduced. (B) Polarized light micrograph of and LC cell created from surfaces assembled orthogonal to each other. The green arrow indicates a region where the top and bottom surfaces were both L-C-L-Y. The angle of the analyzer required to obtain extinction was 2^{o}, indicating loss of twist in the LC cell. (C) Wedge cell created from a $C_{15}SH$ reference surface and L-C-L-Y top surface (green arrow). Scale bar is 2mm.

Maps of Twist Angles of 5CB on L-C-L-Y, L-C-L-F.

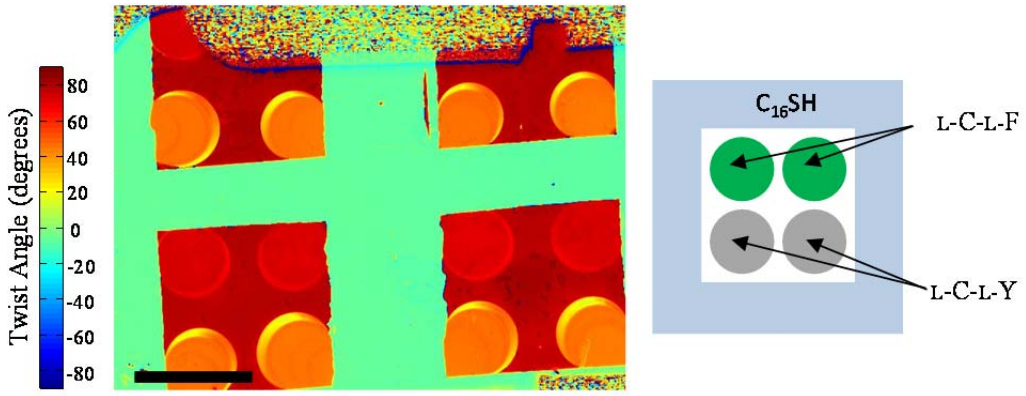

Figure S5. (A) Map of twist angles of 5CB on L-C-L-Y and L-C-L-F. Scale bar is 2mm.

REFERENCES

(1) Lowe, A. M.; Bertics, P. J.; Abbott, N. L. *Anal. Chem.* **2008**, *80*, 2637-2645.
(2) Hostetler, M. J.; Stokes, J. J.; Murray, R. W. *Langmuir* **1996**, *12*, 3604-3612.
(3) Nucci, N. V.; Scott, J. N.; Vanderkooi, J. M. *J. Phys. Chem. B* **2008**, *112*, 4022-4035.
(4) Desamero, R. Z. B.; Kang, J.; Dol, C.; Chinwong, J.; Walters, K.; Sivarajah, T.; Profit, A. A. *Appl. Spectrosc.* **2009**, *63*, 767-774.
(5) Desamero, R. Z. B.; Kang, J.; Dol, C.; Chinwong, J.; Walters, K.; Sivarajah, T.; Profit, A. A. *Applied Spectroscopy* **2009**, *63*, 767-774.
(6) Zinola, C. F.; Rodriguez, J. L.; Arevalo, M. C.; Pastor, E. *Journal of Electroanalytical Chemistry* **2005**, *585*, 230-239.
(7) Roepe, P.; Ahl, P. L.; Gupta, S. K. D.; Herzfeld, J.; Rothschild, K. J. *Biochemistry* **1987**, *26*, 6696-6707.
(8) Hernandez, B.; Pfluger, F.; Adenier, A.; Kruglik, S. G.; Ghomi, M. *J Phys Chem B* **2010**, *114*, 15319-15330.
(9) Uvdal, K.; Vikinge, T. P. *Langmuir* **2001**, *17*, 2008-2012.
(10) Moger, J.; Gribbon, P.; Sewing, A.; Winlove, C. P. *Biochim et Biophys Acta* **2007**, *1770*, 912-918.
(11) Petoral, R. M.; Uvdal, K. *Colloid. Surface. B* **2002**, *25*, 335-346.